Microporous and Mesoporous Materials 194 (2014) 79–82

Contents lists available at ScienceDirect

Microporous and Mesoporous Materials

journal homepage: www.elsevier.com/locate/micromeso

Short Communication

Size evaluation of the fine morphological features of porous nanostructures from the perturbation of heat transfer by a pore filling agent

D. Andrusenko [a], M. Isaiev [a,*], A. Tytarenko [a], V. Lysenko [b], R. Burbelo [a]

[a] Taras Shevchenko National University of Kyiv, 64/13, Volodymyrska Street, City of Kyiv 01601, Ukraine
[b] Institut des Nanotechnologies de Lyon (INL), UMR-5270, CNRS, INSA de Lyon, Universite de Lyon, bat. Blaise Pascal, 7 Av. Jean Capelle, Villeurbanne 69621, France

ARTICLE INFO

Article history:
Received 26 August 2013
Received in revised form 25 March 2014
Accepted 31 March 2014
Available online 12 April 2014

Keywords:
Thermal conductivity
Heat transfer
Porous media
Porous silicon

ABSTRACT

An approach for the size evaluation of fine morphological features of fractal-like porous materials is described. The method is based on the measurements of thermal conductivity of porous layers with empty and filled pore networks. Being associated to a heat transfer model, the experimentally obtained values of thermal conductivity allow the size evaluation of very small structural constrictions ensuring interconnections between the main particles constituting the porous material. The method is applied to determine the size values of the structural constrictions interconnecting silicon nanocrystals forming meso-porous silicon layers.

Complex porous media are known to be quite efficiently characterized in terms of fractal geometry [1]. In particular, fractal-like porous nanostructures contain a large amount of very fine high order features which are often difficult to be clearly visualized or identified. However, these features determine the main physical properties of the nanoscale porous media such as mechanical, heat and charge transports, fluid flows in nano-pores, etc. [1–4]. Porous silicon (PS) nanostructures are certainly among the most prominent examples of such kind of nano-porous media [5]. Indeed, their general fractal morphology was found to govern ac conductivity [6], fluid flows [7] as well as Raman scattering and photoluminescent properties [8]. A special attention is attracted to structural constrictions corresponding to high order fractal features which strongly limit thermal [9] and charge carrier transports [10]. Thus, an independent size evaluation of these features will allow the understanding, tuning and precise prediction of various physico-chemical properties of PS nanostructures as well as interconnected silicon nanoclusters [11].

In this letter, an original concept for the size evaluation of the fine morphological features of porous fractal-like materials is reported. Our approach is based on the introduction of chemically neutral fluid substances inside the pore network and on the comparison of the thermal conductivities of the porous nanostructures before and after the filling of the pores. The perturbation of heat transfer through the porous nanostructure provoked by a fluid (liquid, for example) allows to clearly reveal the determinative role of the fine morphological constrictions in the heat transport and to evaluate their characteristic sizes. Being demonstrated on PS nanostructures, this method can be easily generalized to any other fractal-like solid-state porous medium.

To form 240 μm thick PS layers with 60% of porosity, highly boron-doped p+-type (0.01–0.02 Ω cm) double-side polished (100)-oriented Si wafers were electrochemically treated with an etching solution containing a 1:1 volume mixture of concentrated aqueous HF acid (49%) and pure ethanol. A permanent stirring of the etching solution was applied in order to evacuate hydrogen bubbles formed during the anodization process. Low viscous (20 sPoise) horological oil [12] was chosen as an efficient liquid agent to fill the nanopores. The degree of filling was controlled by gravimetric measurements and reached at least 95% of the total pore volume. The created "PS-oil" nano-composite remained totally stable during the measurements. A monocrystalline Si substrate obtained after the removal of the top PS layer was used as a reference sample.

According to a cross-sectional scanning electron microscopy observation (see Fig. 1a), the PS nanostructures formed on the highly doped p-type Si wafers exhibit a nano-column anisotropic arrangement of Si nanocrystals oriented along the [100] direction and interconnected via fine structural constrictions. Schematic

* Corresponding author. Tel.: +380 988484836.
E-mail address: isaev@univ.kiev.ua (M. Isaiev).

http://dx.doi.org/10.1016/j.micromeso.2014.03.045
1387-1811/

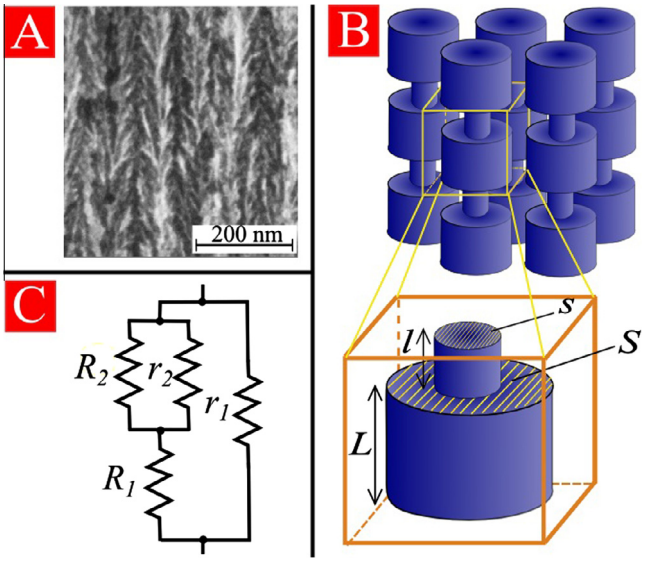

Fig. 1. (A) Typical SEM cross-section view of PS structure; (B) schematic model views of PS nano-columns; (C) the equivalent thermal circuit of the considered PS unit.

model views of the nano-columns constituting the PS layers are sketched in Fig. 1b. In particular, each nano-column can be modeled by a sequence of cylindrical Si nanocrystals with length L and cross-section area S which are interconnected via the fine cylindrical-like constrictions with length l and cross-sectional area s (Fig. 1b). The observed structural anisotropy allows the neglect of lateral interconnections between the nano-columns in comparison with the numerous vertical interconnections between the nano-crysltals forming the nano-columns.

Heat transfer in such PS nanostructures can be quite well simulated by an equivalent thermal circuit represented in Fig. 1c, where: R_1 and r_1 are the thermal resistances of a Si nanocrystal and of the main pore space respectively, while R_2 and r_2 are the thermal resistances of a cylindrical interconnection and its adjacent pore space, respectively. Using the expressions for parallel and series connections of resistors, the expressions for total circuit resistance for empty porous matrix R_{PS} as well as for "porous matrix–liquid" composite R_C are the following:

$$R_{PS} = R_1 + R_2$$
$$R_C = \frac{r_2(r_1R_2 + R_1R_2 + r_1R_1)}{r_1r_2 + R_1r_2 + r_1R_2 + R_1R_2 + r_1R_1}$$

On the other hand, in the frame of the thermal and electricity conduction analogy, it is easy to show that each value of resistance R can be given as:

$$R_i = \frac{1}{\chi_i}\frac{l_i}{s_i},$$

where: χ_i – thermal conductivity of each element, l_i and s_i are the length and cross-sectional area, respectively.

So, thermal conductivities of the PS layers with empty (χ_{PS}) and filled pores (χ_C) can be expressed as follows:

$$\chi_{PS} = \frac{\chi_{n-Si}(1+a)(1-\varepsilon)b}{(a+b)}$$
$$\chi_C = \frac{(\chi_{n-Si}(1+a)(1-\varepsilon) + \chi_l\varepsilon)\cdot(b\chi_{n-Si} + \chi_l(1-b)) + a\chi_l}{(a\chi_{n-Si} + b\chi_{n-Si} + \chi_l(1-b))} \quad (1)$$

where ε is the porosity value, χ_{n-Si} and χ_l are respectively, the thermal conductivities of Si nanocrystals [13,14] and of a liquid filing the porous network, $a = l/L$ and $b = s/S$.

Fig. 2a and b show respectively, the dependences of χ_{PS} and χ_C on the parameters a and b according to the Eq. (1). As one can notice from Fig. 2a, the thermal transport through the as-prepared PS layer with empty nano-pores is mainly limited by the parameter b. Indeed, the very low thermal conductivity values of $\chi_{PS} < 0.5$ W/(m × K) correspond to the values of $b < 0.03$. As for the "PS-oil" composite, its thermal conductivity χ_C never reaches zero (see Fig. 2b) because even for the very low values of b, the heat is transferred via the oil occupying the pore network. For the quite high values of b (close to 0.1), thermal conductivity dependences of both χ_{PS} and χ_C on the parameter a are very similar, showing the highest value (2 W/(m × K)) at $a = 0$ (absence of the structural constrictions between the Si nanocrystals).

The same quantitative and qualitative results are additionally confirmed by a finite-element simulation based on the heat conductivity equation solved in cylindrical coordinates with the origin at the centre of the top surface s. The temperatures at the top (s) and the bottom (S) surfaces, respectively T_T and T_B, are maintained constant. The approximation of zero heat outflows through the side surface is considered. The space distribution of both the flux vectors and isotherms characterizing heat transfer through the PS layers with empty and filled nano-pores can be compared in Fig. 3a and b, respectively. As one can see, the thermal transport in the PS layer with the empty pores is mainly conditioned by the fine solid-state Si constrictions in which the most important temperature gradient is localized (Fig. 3a). The presence of liquid in the nano-pore space results in the appearance of a new heat transfer channel (through the filled pores) between the Si crystallites and, consequently, the isotherms become flatter (Fig. 3b) in comparison with the previous case.

Since the coefficient of thermal conductivity is defined as the proportionality constant between the heat flux density J and the temperature gradient, the effective thermal conductivity values could be evaluated as follows:

$$\chi = -\frac{J}{\vec{\nabla}T} \approx \frac{J(L+l)}{(T_T - T_B)}$$

where an average heat flux J is calculated for simulated nanostructures by FEM. The value of thermal conductivity was found to be very close to the values obtained from the analytical model described by Eq. (1).

The experimentally measured values of χ_{PS} and χ_C will allow estimation of the parameters a and b from the Eq. (1). Measurements of thermal conductivity of the fabricated PS layers were carried out by means of photoacoustic (PA) technique [15] in the configuration of rear surface illumination (open window method) with gas microphone detection [16,17]. As it is shown in inset of Fig. 4, the bottom side of a sample is illuminated by the modulated irradiation of a DPSS green laser module ($\lambda = 532$ nm). The full light power of 0.5 W is quite uniformly distributed over the sample surface so that the power density is found to be about 0.1 mW/cm^2. The photo-excited thermal wave penetrates the sample and causes pressure oscillations of air adjacent to the upper sample surface in the PA chamber. The variable component of the pressure is recorded by an electret microphone. In order to avoid any influence of the sample bending vibrations on pressure variations in the PA chamber (drum effect [18,19]), the bottom surface of the samples was rigidly fixed by a transparent glue to a quartz plate.

In the configuration described above, dependence of the PA signal phase shift ($\Delta\varphi_{PA}$) on the frequency of the light modulation (f) was measured for the following structures: (i) PS layer on crystalline Si substrate; (ii) "PS-oil" composite on crystalline Si substrate; (iii) reference crystalline Si substrate. This phase shift can be presented as a sum of two terms: the first one is the phase shift ($\Delta\varphi_T$) appearing due to the delay of thermal wave propagation

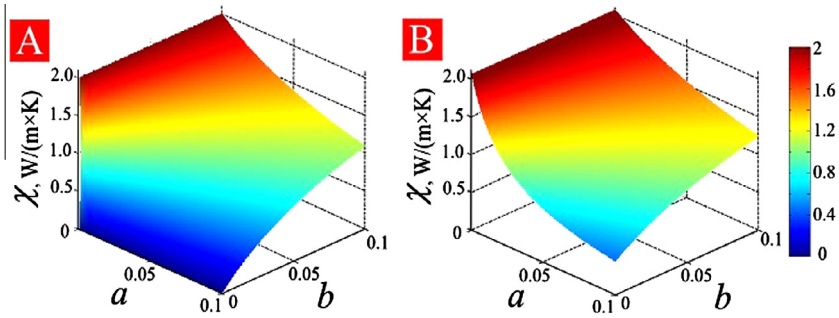

Fig. 2. The thermal conductivity dependences of (A) the as-prepared PS and (B) the "PS-liquid" composite on the fine morphological parameters *a* and *b*.

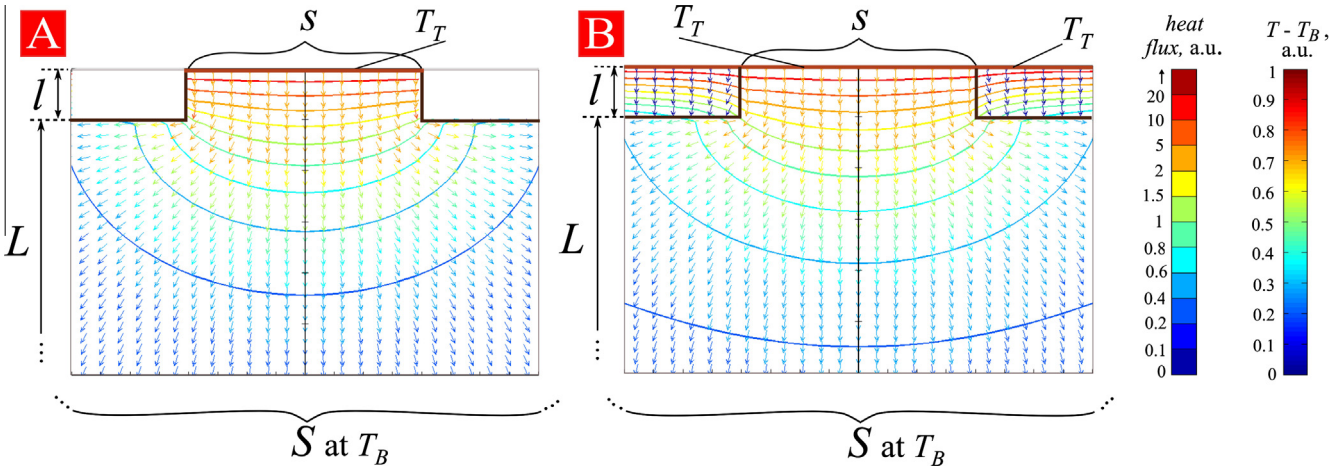

Fig. 3. Spatial distribution of heat flux and temperature in (A) the as-prepared PS and (B) the "PS-liquid" composite.

through a studied sample and the second one is the phase shift ($\Delta\varphi_{instr}$) provoked by the physical parameters of the used PA cell and recording equipment:

$$\Delta\varphi_{PA} = \Delta\varphi_T + \Delta\varphi_{instr}$$

Similarly, for the reference sample (here and below the tilde sign over a function symbol indicates that it concerns the reference sample), one can write:

$$\Delta\tilde{\varphi}_{PA} = \Delta\tilde{\varphi}_T + \Delta\varphi_{instr}.$$

Excluding the $\Delta\varphi_{instr}$ term from the two expressions written above, one can obtain that:

$$\Delta\varphi_T = \Delta\varphi_{PA} - \Delta\tilde{\varphi}_{PA} + \Delta\tilde{\varphi}_T \quad (1)$$

This phase shift results from a time delay of the thermal perturbation going through the porous silicon layer and coming to its bottom sample surface and, therefore, depends on the layer thermal diffusivity. Considering the experimentally measured values of $\Delta\varphi_{PA}$ and $\Delta\tilde{\varphi}_{PA}$, the obtained experimental points of the function $\Delta\varphi_T(f^{1/2})$ determined from Eq. (2) for the (i) and (ii) sample groups are shown in Fig. 4. In order to deduce the thermal conductivity values of the PS layer from this dependence, different calculation approaches can be used (see for example: Refs. [15–18]). In particular, using the exact solution of a 1D heat conduction equation applied to our "PS/Si" and "PS-oil/Si" structures (for example, see Ref. [20]), it is easy to demonstrate that for our experimental conditions, the approximation of a single functional layer (PS in our case) can be efficiently used. This approximation is quite valid in the frequency range for which thermal behavior of the crystalline Si substrate corresponds to a thermally thin layer leading only to the decrease of the PA signal amplitude and to the presence of a constant phase shift. Consequently, for the case of a single homogeneous layer in the frequency range $f > \alpha/h^2$ (where: α is the thermal diffusivity and h is the layer thickness), the following expressions for the phase shift can be used [16]:

$$\Delta\varphi_T(f^{1/2}) = -\pi/4 - h/l_T = -\pi/4 - h/(a/\pi f)^{1/2}.$$

The experimental data in Fig. 4 are very well fitted by this expression. Thus, the thermal diffusivity α of the PS layers can be determined from the slope of the fitting line:

$$\alpha = \pi h^2/p.$$

where p is the slope of the function $\Delta\varphi_T(f^{1/2})$. The thermal conductivities of the PS layers and "PS-oil" composites are calculated from

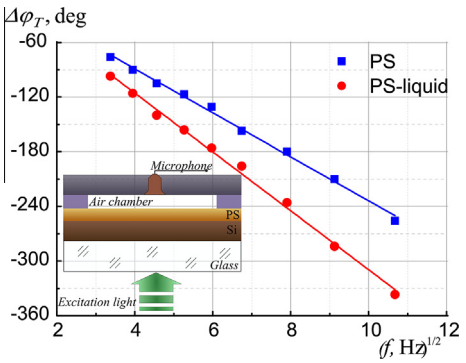

Fig. 4. The dependences of the thermal phase shift of PA signals on the square root of the modulation frequency for the as-prepared PS and the "PS-liquid" composite. Inset: the schematic cross-section view of the used PA cell.

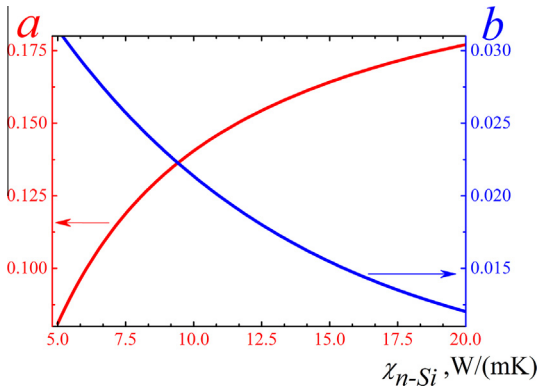

Fig. 5. Morphological parameters a and b as functions of the thermal conductivity of Si nanocrystallites χ_{n-Si}.

the following equation: $\chi_{PS,C} = c_{PS,C}\rho_{PS,C}a_{PS,C}$, where c and ρ are respectively the specific heat capacities and volume densities of the PS and "PS-oil" composites. The products $c_{PS}\rho_{PS}$ and $c_C\rho_C$ are calculated according to the following relations:

$$c_{PS}\rho_{PS} = c_{Si}\rho_{Si}\cdot(1-\varepsilon)$$
$$c_C\rho_C = c_{Si}\rho_{Si}\cdot(1-\varepsilon) + c_{Oil}\rho_{Oil}\cdot\varepsilon\cdot\xi$$

where $c_{Si,Oil}$ and $\rho_{Si,Oil}$ are, respectively, the specific heat capacities and volume densities of bulk crystalline Si and oil, $\varepsilon = 0.6$ is the volume porosity of the PS layers and $\xi = 0.95$ is the degree of pore filling by oil.

The thermal conductivity values of the PS samples and "PS-oil" composites were determined from the experimental procedure described above and they were found to be equal to: $\chi_{PS} = 0.60 \pm 0.04$ W/(m × K) and $\chi_C = 0.94 \pm 0.06$ W/(m × K), respectively. The enhanced values of χ_C in comparison with χ_{PS} can be explained by the enhancement of the heat transport between the interconnected Si nanocrystallites due to the oil filling the porous network. By substituting these experimentally obtained thermal conductivity values in the expressions (1), the obtained system of equations allows the determination of the unknown parameters a and b characterizing the fine morphological features of the PS layers. Typical range of values of these parameters are given in Fig. 5 for different thermal conductivity values (χ_{n-Si}) of Si nanocrystallites constituting the PS layer. In order to determine the absolute values of l and s of the structural constrictions, one has to estimate the values of L and S by Raman scattering spectroscopy or XRD measurements [21,22].

In conclusion, the measurements of the thermal conductivity of porous layers with empty and filled pore networks associated to a heat transfer model allow the size estimation of the fine structural features determining main physical properties of the studied layers. This approach gives additional information on the morphology of porous materials which is difficult to be obtained in another conventional way. Being demonstrated on PS nanostructures, this method can be easily generalized to any other fractal-like solid-state porous medium.

References

[1] P.M. Adler, J.F. Thovert, Trans. Porous Med 13 (1993) 41.
[2] I. Srivastava, S. Sadasivam, K.C. Smith, T.S. Fisher, J. Heat Transfer 135 (2013) 061603.
[3] J.H. Cushman, Water Resour. Res. 27 (1991) 643.
[4] B. Yu, Appl. Mech. Rev. 61 (2008) 050801.
[5] T. Nychyporuk, V. Lysenko, D. Barbier, Phys. Rev. B 71 (2005) 115402.
[6] M. Ben-Chorin, F. Möller, F. Koch, W. Schirmacher, M. Eberhard, Phys. Rev. B 51 (1995) 2199.
[7] V. Lysenko, J. Vitiello, B. Remaki, D. Barbier, Phys. Rev. E 70 (2004) 017301.
[8] M. Wesolowski, Phys. Rev. B 66 (2002) 205207.
[9] P. Chantrenne, V. Lysenko, Phys. Rev. B 72 (2005) 035318.
[10] V. Lehmann, F. Hofmann, F. Möller, U. Grüning, Thin Solid Films 255 (1995) 20.
[11] T.G. Desai, Appl. Phys. Lett. 98 (2011) 193107.
[12] Russian GOST-7935.
[13] N. Mingo, L. Yang, D. Li, A. Majumdar, Nano Lett. 3 (2003) 1713.
[14] C. Abs da Cruz, K. Termentzidis, P. Chantrenne, X. Kleber, J. Appl. Phys. 110 (2011) 034309.
[15] D.V. Bageshwar, A.S. Pawar, V.V. Khanvilkar, V.J. Kadam, Eur. J. Anal. Chem. 5 (2) (2010) 187–203.
[16] P. Korpiun, B. Merté, G. Fritsch, R. Tilgner, E. Lüscher, Colloid Polym. Sci. 261 (1983) 312.
[17] M.J. Adams, G.F. Kirkbright, Analyst 102 (1977) 281.
[18] R. Burbelo, D. Andrusenko, M. Isaiev, A. Kuzmich, Arch. Metall. Mater. 56 (2011) 1157.
[19] A. Somer, F. Camilotti, G.F. Costa, C. Bonardi, A. Novatski, A.V.C. Andrade, V.A. Kozlowski, G.K. Cruz, J. Appl. Phys. 114 (2013) 063503.
[20] D. Andrusenko, M. Isaiev, A. Kuzmich, V. Lysenko, R. Burbelo, Nanoscale Res. Lett. 7 (2012) 411.
[21] M.N. Islam, A. Pradhan, S. Kumar, J. Appl. Phys. 98 (2005) 024309.
[22] R.J. Martin-Palma, L. Pascual, P. Herrero, J.M. Martinez-Duart, Appl. Phys. Lett. 87 (2005) 211906.